Project NoScope

Mark Hardiman
Ying Ou
Ryan Frazier
Zeyi Lee
Longxiang Cui
Laura Waller, Ed.
Ming C. Wu, Ed.

Electrical Engineering and Computer Sciences
University of California at Berkeley

Technical Report No. UCB/EECS-2015-51
http://www.eecs.berkeley.edu/Pubs/TechRpts/2015/EECS-2015-51.html

May 9, 2015

Acknowledgement

I would like to thank Dr. Laura Waller, this capstone's project advisor, for her constant helpfulness and for her insightful project idea. It was a pleasure working with her. Furthermore, thanks to Dr. Ming Wu for his help and advice while reviewing this report.

University of California, Berkeley College of Engineering

MASTER OF ENGINEERING - SPRING 2015

Electrical Engineering and Computer Science

Signal Processing and Communications

Computational 3D Microscope

MARK HARDIMAN

This **Masters Project Paper** fulfills the Master of Engineering degree requirement.

Approved by:

1. Capstone Project Advisor:

Signature: _____ Date _____

Print Name/Department: LAURA WALLER/EECS

2. Faculty Committee Member #2:

Signature: _____ Date _____

Print Name/Department: MING WU/EECS

ABSTRACT

This project report covers the development of a computational 3D microscope, NoScope. Using tomographic and light field algorithms, we present a method to reconstruct 3D volumes of microscopic samples taken with a lensless sensor. Business and intellectual property strategies for commercializing NoScope are detailed in the first three sections. The remaining sections highlight the project's technical accomplishments and methods.

Capstone Report
Project NoScope

Mark Hardiman

A paper submitted in partial fulfillment of the
University of California, Berkeley
requirements of the degree of
Master of Engineering
in
Electrical Engineering and Computer Science

May 2015

Contents

Part I

Problem Statement

1 Project Introduction

As technology has advanced with the emergence of digital computing and signal processing, computers that used to take up entire rooms now fit in a backpack, and doctors and nurses have diagnosis equipment built into their cellphones. However, the optical microscope, a piece of equipment crucial for any medical or experimental lab, has remained unchanged for nearly three hundred years. Modern commercial microscopes rely on fragile lenses and precise alignments, and without additional equipment have no means of sharing the acquired images. Heavy and bulky, they are living fossils in a portable world and would benefit greatly from a technological overhaul.

Many fatal diseases, such as malaria, are endemic in tropical areas around the world. In order to better cure people with such diseases, a faster and more affordable detection and diagnosis method is greatly needed in those region. Traditional microscopes had reached their ceiling of being portable due to its fragile nature, and thus cannot be used as a means to diagnose diseases in the field. A more portable device is needed for doctors and nurses working in those area. With a faster diagnose method, millions of lives will be saved every year.

Imagine a world in which the advantages of microscopy are readily available to every individual with a need due to a low price and viability in a wide range of environments. Furthermore, the microscopic images may easily be made digital. Has a boy in a small African village contracted malaria? How can a doctor in a distant area assess over the Internet a patient's health whose disease requires microscopy? These questions find an answer in a robust, inexpensive, and yet powerful digital microscope. Additionally, people everywhere would be free to explore an exciting and useful unseen world.

How can we achieve our vision then? The clue lies in the advent of digitization and higher computational power; we believe these two factors should be the driving force in future of microscopy. Unlike traditional optics, constrained by the limits of the physical world, computational microscopy can ride the tide of improving electronics, compensating for lack of expensive optics with more complex, but more cheaply achievable computations. In particular, the availability of memory and modern processing speed on common consumer devices opens up access to image-processing algorithms that were previously privy to only the world of laboratory work.

As such, our team wishes to leverage the broader trend of digitization to develop a robust, cheap, portable diagnostic tool that can produce digital images of traditional medical samples. With its advanced computational imaging processing technologies, the NoScope manages to create high-resolution digital images without optical lenses. Abandoning the expensive and fragile lenses, NoScope successfully eliminates the high cost and special handle requirement associated with lenses. In addition, since samples are imaged by USB cameras, the digital files can be shared among individuals easily.

Part II

Capstone Strategy

Contents

1 Introduction

By the end of April 2015, the goal of Team NoScope is to produce a minimum viable product of a prototype microscope that creates three-dimensional images of microscopic samples. We plan on accomplishing this through a series of computational algorithms combining principles of limited angle tomography (Kak et al., 1988) and light field imaging (Levoy et al., 1996). Using these imaging techniques, our hardware will create a three-dimensional image from a series of two-dimensional ones. The goal of this paper is to give the reader a brief introduction to our product, then explain its necessity in the market through its key value propositions, and finally elucidate our strategy for entering the congested microscopy market.

1.1 Our Product

The end goal of project NoScope is a fully functioning, robust microscope prototype that can be taken to market as a minimum viable product. The main factors driving our hardware development are portability, durability, and low cost. In order to limit cost, our team has developed a lensless system that bypasses the need for expensive and fragile lenses, which builds upon the LED array illumination technique in Waller Lab (Tian et al., 2014). We have also incorporated a simple microcontroller on the device, allowing the intensive computations to easily be performed by an attached computer. This significantly reduces the number and complexity of parts, when compared to a traditional microscope.

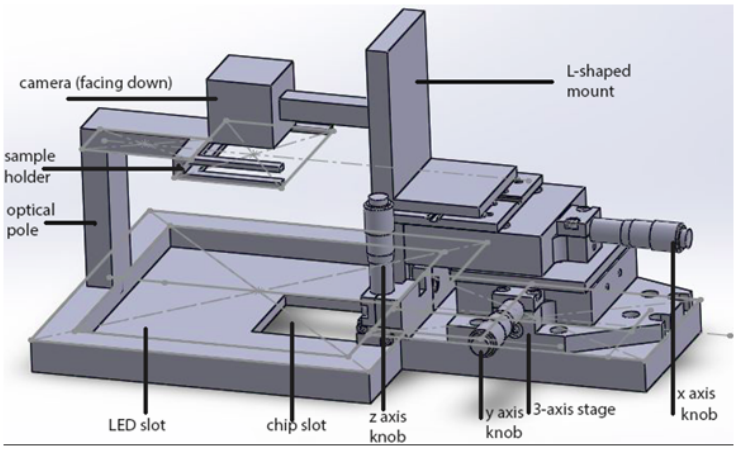

Figure 2.1: Isometric view (CAD) of NoScope.

The current iteration of NoScope consists of a 32x32 matrix of LED's, a camera sensor, and a microcontroller that synchronously triggers specific LED's with camera exposures. During prototyping a custom designed, 3D printed case will house the components. By connecting to a laptop and running software we are developing in parallel with the hardware, the end user will be able place samples on a standard microscope slide and acquire high-resolution 3D images. The inclusion of light field algorithms allows the image to be refocused in post-processing so that various depths of the image can be analyzed by the end user.

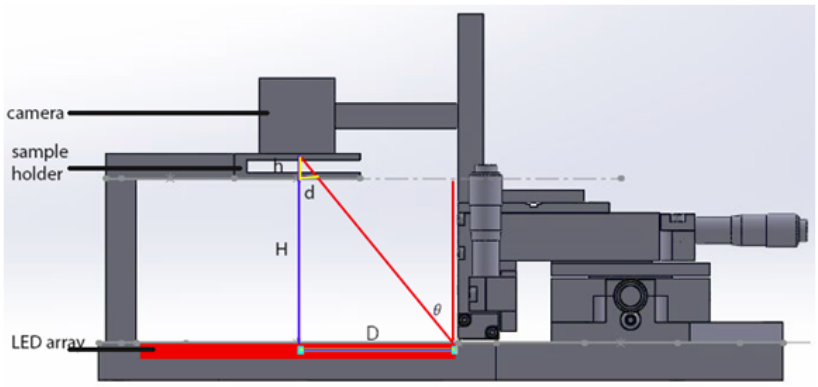

Figure 2.2: Side view hardware schematics of NoScope. Notice the distance of the sample holder to the camera.

Note that figure 2.2 shows the sample placed extremely close (approximately 2mm) away from the camera sensor. This configuration hints at the fundamental working principle of NoScope: casting a shadow of the sample on the sensor. By illuminating a translucent sample, we project an image of the sample on the sensor. Since modern sensors have extremely small pixel pitches (distance between pixel), we are effectively able to view images of its shadow at microscopic scale, thus acting as a microscope. For example, our sensor has a pitch of 5.3μm.

In addition, we are able to generate different 'views' of the sample by illuminating different LEDs. Since each of the LEDs are placed at a different angle incident to the sample, lighting different LED, and taking separate exposures is analogous to viewing an object at different angles. This also forms the basis for digital refocusing.

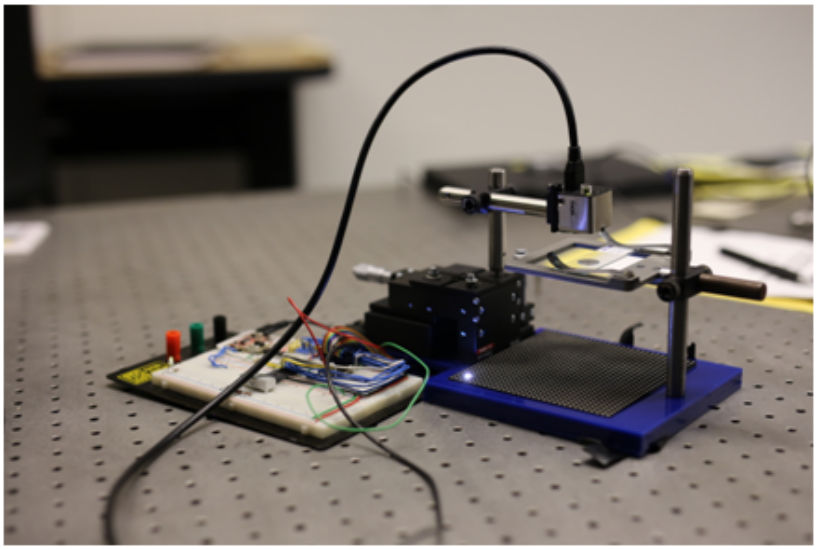

Figure 2.3: First iteration of NoScope. The breadboard is a temporary module and not an actual part of the prototype.

For the current iteration of NoScope, we were able to achieve a resolution of about 32 lp/mm, as well as resolve 3D structures of various microscopic specimens using light field methods. More details can be found in the technical contribution section.

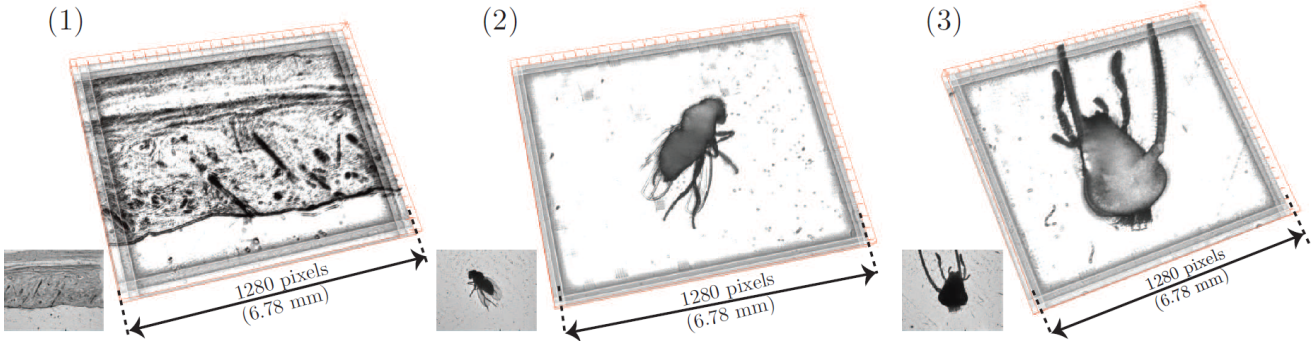

Figure 2.4: Examples of 3D samples from Light field algorithm. No thresholding/post-processing applied. Taken from light field technical contribution report (Lee, 2015).

While the current resolution we can achieve with NoScope is still slightly low, the resolving power of a lensless microscope can be improved by using a sensor with smaller pixel pitch, and better algorithms to account for wave effects. We envision future iterations of NoScope to be used for diagnosing diseases as well as for academic use in teaching environments. In addition, our product can also potentially replace pricey optical microscopes as an inexpensive alternative.

2 Need for Product

Commercialization of NoScope requires the identification of the customers and a full understanding of their needs. In order to find our potential customers, this section will first examine the broader trends in the microscopy industry, and identify a niche for NoScope. Then it narrows down to a specific primary stakeholder and discusses their potential needs, and how these can be fulfilled by NoScope. It further shows that this potential need has not been fulfilled by other products, by analysing the difference between NoScope and our close competitors. Accurate identification of the customer's needs helps companies to shape strategies and have a better positioning. Therefore, this section lays a concrete foundation for our marketing strategy to be discussed in the subsequent section.

2.1 Motivating Trends

As an intrusive new entry, NoScope expects to assist the technology revolution in microscopy and to fulfill needs for underrepresented customers. This section identifies the motivating trends for our microscope in the general industry and our primary market.

Microscopy is a fast growing industry. The market revenue is expected to double in five years from 3.84 billion in 2014 (IndustryARC 2013, p.11). The growing market along with the unique features of NoScope could lead to future investment in NoScope. In addition, this industry is also experiencing a technological shift. The traditional optical microscopes are gradually losing favors due to the limited resolution (IndustryARC 2013, p.13). NoScope might be able to help optical microscopes to regain popularity. The core technology of NoScope is the 4D light field imaging, which is designed to increase the resolution of the sample images without optical lenses. Once this technology has proven to be applicable, it will be possible for NoScope to lead other optical microscope companies to further increase the resolution of optical microscopes.

Despite the industry's maturity, current microscopy still cannot fulfill all its customers' needs. Aside from the expensive cutting-edge equipment being produced by leading companies in this field, there is a significant need for a low-cost product. One particular example is the use of microscopy in malaria diagnosis. According to World Health Organization (WHO), the funding for malaria control and elimination has reached US 2.7 billion by the end of 2013, a threefold increase since 2005, and this

growth of funding has been greatest in Africa Region (WHO 2014, p.12). However, this funding falls far below the 5.1 billion that is required to achieve global targets for malaria control and elimination (WHO 2014, p.12). Replacing expensive microscopes with NoScope can potentially save thousands of dollars for medical facilities, which allows more funding to be channeled into prevention and treatment of malaria.

2.2 Satisfying Stakeholders in Medical Diagnosis

Moving further along the argument of a potential niche in malaria diagnosis, we have thus identified our primary stakeholders as doctors, or medical technicians in malaria-endemic areas. By the end of 2015, there will be about 1 million community health workers in sub-Saharan Africa, estimated by researchers in Columbia University (Singh et al., 2013). However, doctors and nurses alone are not enough to solve the problem. According to WHO, there were about 207 million cases of malaria in 2012 and an estimated 627,000 deaths (WHO 2014b). In order to contribute to the fight against tropical diseases in under-developed regions, we plan to provide these health workers inexpensive and portable microscopes with strong disease diagnosis ability.

The biggest challenge for us is maintaining a low price point. Governments of developing countries cannot afford sufficient expensive medical equipment to satisfy diagnostic needs. On the other hand, doctors from nonprofit organizations mainly rely on donations from external parties, and also have limited budgets. Therefore, expensive microscopes–which are in the range of thousand dollars–are not suitable for our primary customers.

Our key value proposition is thus to make our hardware highly affordable by using a lensless design. Microscopy lenses are particularly expensive, comprising the majority of a typical microscope's price. Naturally, by avoiding lenses altogether, we can significantly reduce our selling price. This allows our customers to have more money to invest in disease treatment rather than diagnosis.

Our second value proposition is portability and robustness. It is no coincidence that many of the malaria-endemic areas, such as North India, and Africa, are also less economically developed. Consequently, these regions may lack proper transport infrastructures. The conventional microscope lens is a piece of equipment that not only is heavy, but also fragile. As such, these lenses often come with their own protective suitcases. These logistical factors further compound the difficulty of getting

the microscope to the field. By removing the lens entirely, we address the issue of accessibility of microscopic diagnostic services by transforming the microscope into a light, electronic device.

In addition to being lensless, NoScope boasts a unique feature of 3D imaging. The ability to view samples in 3 dimensions can help increase the accuracy of disease diagnosis. Most disease diagnosis relies on morphological discrimination of unhealthy cells based on pathological features (Tadrous, 2011). A 3D image allows doctors to view the sample from different angles, and observe features that might otherwise be hidden in 2D projections or slices. This leads to higher accuracy identification of cell types or parasites. Incidentally, as the following section will show, the 3D imaging feature also distinguishes us from the rest of our competition, making NoScope the most suitable product for disease diagnosis.

2.3 Differentiation: NoScope vs Competitors

In the process of selecting our closest competitors, we have considered the similarity of their technology to ours, as this is a good indication of how directly they compete against NoScope. Building on this, we have further subdivided our competitors coming from the industry and academia. On the commercial side, this section will cover our potential rivals from Lytro, Cellscope, and Pelican. In academia, we will examine the field-portable tomographic microscope by Ozcan Research Group in UCLA.

In comparing our product with those of the competition, we keep in mind the key criteria of cost, portability, and computational imaging capabilities–particularly any 3D capabilities. Although the products of these competitors may hold some advantages over our product in certain areas, NoScope still holds its weight in the market of lightweight, inexpensive imaging systems for disease diagnosis.

Competition in the Industry

In this subsection, we evaluate three industry competitors: Lytro, Cellscope, and Pelican Imaging.

Lytro

We start our industrial competitor analysis from the computational imaging system developed by Lytro. This system is marketed toward everyday users who want to capture depth-related details in their life photos and have more post-processing options available to them to modify these photos. The system boasts a small form factor that makes it convenient to be carried around without hassle. The

light sensor array requires lenses to properly focus the light for capturing light-field information. This light-field technology enables Lytro to vary parameters such as depth-of-field as well as numerical aperture in post-processing (Lytro, 2015), which is a large factor in the appeal of computational imaging systems. However, the method of computational imaging at work in their product does not allow for high-resolution 3D images due to the poor range of angles available to a camera in a macroscopic scene. Most importantly, Lytro does not focus on disease diagnosis and is incapable of microscopy, and thus fills a different need in the imaging market compared with our target customers.

Cellscope

Cellscope offers strictly an optical assembly to accompany a user's smartphone to allow for convenient microscopy while taking advantage of computing power and hardware already in the user's possession. Their product consists of a mount for a smart phone, mirrors and lenses, and a mount for the specimen to be viewed. In concert with a smart phone, this assembly accomplishes the key points of being lightweight and affordable while allowing for taking microscopic images. (Cellscope, 2015) Despite these advantages, Cellscope does not offer computational imaging, and thus has no capability of creating 3D images, which renders it less useful in garnering detailed information about samples, such as malaria parasites.

Pelican Imaging

Pelican Imaging has developed–but has yet to sell or contract out use of–a computational imaging sensor capable of replacing the camera in future smart phone models. The capabilities of a smartphone with this type of integration exhibit much similarity with those of Lytro cameras, particularly post-processing to alter many key characteristics of photos. Hence, we find that Pelican's sensor module matches up against our product in much the same way as Lytro does. However, there is potential for a future product combining Pelican's sensor module as Cellscope to fill the same market need as our product. Such a combination would combine the advantage of 3D imaging with portability and microscopy (Anderson, 2015). However, the optical components present in Cellscope's product may put the price point higher than our product. This combination would also rely on the user to already have a smartphone with Pelican's sensor.

Although this competition in still theoretical at this point, it indicates that there is movement toward filling this niche in the market that we are targeting, and thus informs us to move quickly in developing

our product to gain hold of the market.

Competition in Academia

Field-portable Tomographic Microscope - UCLA

Looking at our academic competitor, Ozcan Research Group in UCLA has a design that bears many similarities to our proposed design. Namely, their microscope employs an LED array, as well as a lensless design, both of which are also key features in our device.

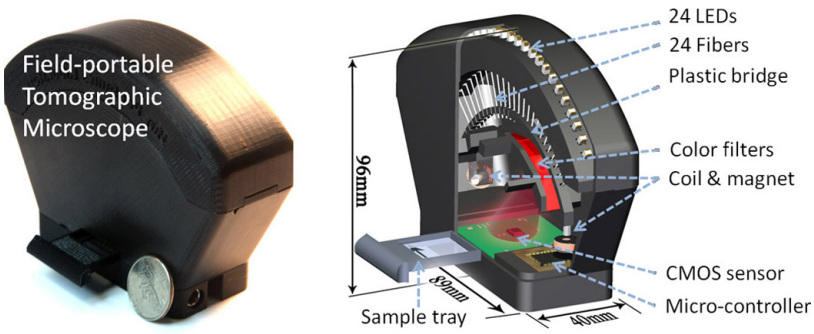

Figure 2.5: The schematics of Ozcan Research Group's tomographic microscope.
[Image Source: `http://www.spie.org/x84293.xml`]

Their image processing technique also resembles ours on the surface. Using multiple angles of illumination, their device takes images of the same specimen at different angles. In addition, in order to extend the angles of illumination beyond one axis, the coil and magnet in the device can electrically actuate the optic fibers to light the sample differently, giving the device an additional axis of data to work with. Following which, the on-board chip on the microscope processes these images into a 3D hologram using the technique of dual-axis tomography (Isikman et al., 2011).

A closer examination reveals several differences between the two devices. In terms of image processing, we are currently tackling the problem using two approaches: 4D light field, as well as 3D tomography. For the more comparable tomography technique, our device differs by virtue of the number of LED axis we have. By employing a full 2D matrix of LEDs, as opposed to just two axes in their device (additional axis by driving coils), our design endows us with multiple axes of data to work with. Consequently, we expect to be able to achieve a higher theoretical fidelity when it comes to reconstructing the 3D structure.

Aside from the algorithm used, we expect our device to be far lower cost than UCLA's microscope, owing to the simplicity of our design. The first reason is that the domed-shaped housing for the LED, which has to be custom made, is much more expensive than a flat piece of LED array we are planning to use, which can be bought off-the-shelf.

Additionally, UCLA's microscope achieves their second axis of illumination by actuating magnetic coils on the device (Isikman et al., 2011). This undeniably adds complexity, and hence cost, to the device. In contrast, as mentioned in the analysis of our tomography algorithm, the nature of our 2D LED array already allows us to have multiple axes of illumination. Taken together, we expect our device to be simpler in design, but still capable of achieving the same, if not better, resolving capability.

From our analysis of competitors above, we find our product provides a service not yet filled by others. Although Lytro, Pelican Imaging, Cellscope and Ozcan's Research group have somewhat similar products, our end goal will serve a need separate from all of them by providing a portable, low-cost microscope capable of 3D imaging focusing on disease diagnosis.

Since we accurately identified the specific need of our stakeholder, we are better able to differentiate ourselves from our competition. As such, we have laid the foundation of a specific need we hope our product will eventually be able to satisfy. The following section will thus use that niche as an anchor to expand on the broader strategy of entering the market.

3 Entering the Market

Successful entrance into our target microscopy market necessitates an overall understanding of the forces and trends permeating this market. In this analysis, we aim to garner insight regarding those technological and business aspects that impact our strategy to enter the market, which include profitability under competitive forces, and the pricing of our product.

3.1 Competitive Forces Analysis

We first seek to gain a thorough understanding of the factors affecting profitability in this market. In evaluating these factors, we apply Michael Porter's well-known framework of the "Five Forces" model to gauge competitive forces. We further consider positioning ourselves according to Clay Christensen's "disruptive innovation" model in order to help combat each of these forces.

As this technology has not yet been commercialized in the application of microscopy, considerable opportunity exists in the market for our product. However, we find the current industry environment hostile to new entrants such as ourselves, and we must overcome strong barriers to entry in order to gain a foothold in the market. Substitutes for our chosen application of malaria diagnosis–medical diagnosis and Rapid Diagnostic Test RDT–pose a threat of luring customers away from our product. Finally, we consider what power buyers and supplier might have over our profitability in this market.

Established Rivals

A small number of large companies command most of the power and profit in the microscopy industry; indeed, more than 90% of revenue in the $5,682 million industry of 2013 went to a limited number of key players (McWilliams, 2013, p. 135). Looking at industry reports, we find that these key players largely consist of glass manufacturers (Uba, 2015, p. 14). The clout of this cluster of glass manufacturers presents a considerable barrier to entry due to the limited number of suppliers. However, since a large advantage of the technology we employ is the lack of optical components such as lenses, we expect to be minimally affected by the clout of this cluster of glass manufacturers. This allows us to circumvent the strong barriers to entry set up by the larger players of the industry.

Established microscope companies have more resources and better reputation than we would upon

entering the market. How then can we penetrate the market to become profitable while minimizing retaliation from incumbents? The answer lies in Clayton Christensen's "disruptive innovation" model. By taking advantage of the un-catered needs of markets with lower gross margins, we can reach a customer base with a smaller budget and thus enter the market (Christensen, 2015, p. 1). The lensless nature of our system brings our costs low enough to be highly competitive, and undercut the cost of microscopes with similar specifications, as we discuss in the next section on pricing. Large microscope companies will run the risk of degrading their profits in order to compete on a similar price point.

Furthermore, our technology presents its own barrier to mimicry. After searching through commercially available options, we found that computational imaging has not yet been commercialized for any microscope, so companies would be forced to conduct R&D in the field of our technology in order to take advantage of the value that saves product cost. Lastly, even if competitors increase the R&D effort for a comparable product, they run the risk of self-competition. The customer bases between our initial customers and a typical microscope producer are not mutually exclusive; these competitors would compete with their own products for the same customers if they chose to mimic our technology.

Buyers and Suppliers

The buyers of microscopes come from various industries. The life science industry is the largest player on the buyer side with 26% of the market, followed by the semiconductor industry, education, and the nanotechnology industry, with market share as shown in Table 1 below (McWilliams, 2013, p. 7).

Table 2.1: Global microscopes market share by major application, 2012 (McWilliams, 2013, p.7).

Industry	**Proportion of Market**
Life science	26%
Semiconductors	24%
Education	12%
Nanotechnology	7%

From Table 1, we can clearly see that the life science industry is the biggest player in the buyer's side, but it does not dominate the market. The semiconductor industry and material science industry both have similar market shares as the life science industry on the buyer side. Furthermore, if we look into

the life science industry, microscopy has been the de facto tool of cell and tissue analysis from 1800 (Rosen, 2005), and it is extremely hard for the industry to find substitutes for the microscope and change its 200 year-old habit. Therefore, we can safely conclude that the buyer power of microscopy industry is relatively weak.

If we look at the components of a microscope, its most expensive and fragile parts are the lenses. Looking at the major supplier microscopes, the optical instrument industry, we find an interesting phenomenon–the major players in the microscopy industry, such as Nikon and Carl Zeiss Ag (McWilliams, 2013, p. 135), also have business in optical instrument manufacturing industry (Oliver, 2015; Uba, 2015). This shows that the suppliers of large microscope companies are themselves; these companies most likely found it profitable to perform backwards integration by bringing manufacturing in-house. The supplier power is thus weak for the large companies in the industry. However, this also means small companies and OEMs in the industry need to buy lens from their major competitors. The supplier power for small companies in the industry is quite high. In order to mitigate the strong supplier power from those big players, we designed our product to be lensless. The electrical components of our product, a LED array and a CCD camera, are easily replaceable. Therefore, we can conclude that the supplier power for our product is also relatively weak.

Threat of Substitutes

Next, we consider the power of substitutes for diagnosis of malaria by evaluating the two major substitutes: clinical diagnosis and Rapid Diagnostic Test (RDT). We show that microscopy remains the de-facto gold standard for diagnosing malaria, and hence, the threat of substitution is weak.

Plasmodium is the malaria-causing parasite. Conventional diagnosis of malaria works by staining a patient's blood smears using a mixture of acidic eosin and methyl blue, known as Giemsa's solution. (Fleischer et al., 2004, p. 2). This solution stains the *Plasmodium* infecting red blood cells, allowing technicians to detect their presence under a microscope.

Unfortunately, the microscope has its limitations; financial and technical obstacles combined preclude microscopy from being more widely used. Current microscopes are inherently bulky and expensive. Furthermore, the typical optical microscope requires a trained technician to operate, increasing the difficulty of getting a good microscopy test in poor rural regions.

In spite of that, medical experts widely consider Giemsa microscopy to be the most reliable method for diagnosis (Murphy et al., 2013, p. 2). This is due to its low per-use cost, at approximately USD $0.12 0.40 per smear (Wongsrichanalai et al., 2007, p. 6), and its ability to quantify accurately, the severity and variant of *Plasmodium* in the blood sample. This is also the reason why we have targeted malaria diagnosis as our initial market; our simpler lensless microscope can increase the accessibility and affordability of good microscopy service in this much needed market.

Clinical Assessment

We now consider the most basic form of diagnosis: clinical assessment by a doctor. The process of clinical diagnosis starts with recording a patient's travel history. More specifically, this considers any high-risk endemic area in a one-year window prior to diagnosis, such as Africa, North Korea, or North India. However, this has the flaw of assuming an accurate travel history. In addition, the highly variable incubation period across *Plasmodium* variants means that, in some cases, even a one year period is not enough to cover all bases. For example, the vivax variant of *Plasmodium* found in North India and Korea will only start attacking the body 12-18 months after the mosquito bite (Griffith et al., 2007).

Moreover, even after establishing the travel history, recognizing malaria infection based purely on symptoms is not straightforward. Early symptoms of malaria bear many similarities to other common diseases, such as fever, chills, headache, and malaise. Inevitably, this complication hampers the early diagnosis of malaria, especially when it is at its most treatable stage. Unfortunately, it is only in the later stages in which the most telling, but fatal, symptoms surface. These includes coma, anaemia, hypoglycaemia, and more (WHO, 2010, p. 4).

Ultimately, diagnosis itself cannot provide confirmation of malaria infection. This implies that most clinical diagnosis will invariably fall back on microscopy as a final step. Naturally, it seems reasonable to deduce that pure clinical diagnosis is a weak substitute for giemsa microscopy.

Rapid Diagnostic Test

The next best alternative is known as Rapid Diagnostic Test (RDT). RDTs are dipsticks which indicates the presence of antigens (proteins) secreted by *Plasmodium* in the blood. A patient uses a RDT by pricking a small amount of blood on a test strip containing antibodies targeting specific *Plasmodium* antigens. Depending on the result, the blood colors the test strip in a specific manner, allowing

a quick diagnosis.

Figure 2.6: Example of a Rapid Diagnostic Test, BinaxNOW from Alere. Source: `https://ensur.invmed.com/ensur/broker/ensurbroker.aspx?code=12000304&cs=26232437`

The advantage of using RDT is that it is fast and easy to use. Unlike a microscope, the small RDT test kit can be brought out to the field, and be used by an untrained person by reading off the strip. It also does not require an electricity source. Most importantly, the RDT can give an indication within 5-20 minutes, making it suitable for screening a larger number of people. This also accounts for its recent popularity. These tests are increasing in popularity and use in recent years, with 319 million units of reported sales in 2013, up from 46 million in 2008 (WHO, 2014, p. 22).

Despite its popularity, RDTs remain far from being a microscopy replacement. The first issue is that RDTs are only sensitive towards one variant of *Plasmodium*, the falciparum. For other variants, the RDT becomes less sensitive, especially when parasite density is low (Wongsrichanalai, 2007). This opens up the danger of false negatives. Second, the RDT is unable to distinguish between variants of *Plasmodium*, which is essential for effective treatment. Third, RDTs cannot quantify the concentration of the parasite in the blood, which indicates the severity of infection.

The limitations of RDT put it, at best, a complementary product, rather than a substitute, for microscopy. It is currently well-suited for giving quick diagnosis in areas where microscopes or technicians are unavailable.

Having considered the available substitutes, we believe NoScope attacks a sweet spot in the space of diagnosis by offering diagnostic reliability, accuracy, ease of use (no optical focusing), and affordability. By carefully segmenting an application of microscopy that has no viable substitutes, we have positioned our lensless microscope in a strategically strong position. As such, a vital specification of our microscope is to be able to resolve the *Plasmodium* variants, as well as doing it affordably, in order to

place ourselves in an advantageous position in the malaria diagnosis market.

Upon examining the competitive forces in our chosen market, we expect to encounter strong barriers to entry. We can circumvent profit loss by taking advantage of the lensless nature of our system. This lack of optical components also contributes to our highly competitive price point, which fuels our use of the disruptive innovation model of entering a market. Large companies ultimately would not provide strong retaliation due to factors of price point, R&D costs, and self-competition. We find buyer power weak due to the large demand for microscope and the unique value of NoScope. Supplier power does not dampen profitability considerably due to the interchangeability of suppliers that our system design affords us. Our affordable and powerful design is highly competitive against the available substitutes. Altogether, we expect these competitive forces to weigh little against our potential profitability.

3.2 Competitive Pricing in a Saturated Market

While the previous section covered the broader business strategy, this section will cover our specific competitive pricing tactics for NoScope. Too low of a price will hurt profits and will not allow us to expand quickly. Too high of a price, however, would put us in direct competition with large microscope producers whose brand recognition and R&D power we cannot match.

The Top-down Approach

To determine the optimum price, we used a top down approach and analyzed Nikon's annual shareholder report. As one of the leading microscope producers, Nikon's 2013 net sales for optical instruments was 41.9 million dollars (Nikon, 2013). At an average cost of $530 per microscope, calculated using `http://amscope.com`'s inventory, this comes to 79,056 units sold per year. Our team wants NoScope to have a 5 year first-generation life cycle with one year of R&D Preceding. Being a smaller startup, our expected sales per year were determined as a fraction of Nikon's annual sales, with expected sales approximately doubling each year as the company grew.

The Bill of Materials for NoScope was calculated using reputable vendors such as DigiKey. This in combination with employee costs was used to calculate annual sunk costs (Figure 2.3). Using this data, we determined that in order to turn a profit on NoScope after three years we would need a product cost of $120.60. Calculating a 50% buffer for unexpected costs leads to a final price tag of $189.99 per unit. This is well below the average traditional microscope cost allowing us to compete with

established rivals price-wise, while still remaining competitive in the event of new market entrants.

Figure 2.7: Accumulated costs vs. units sold for product lifecycle

As mentioned above, we estimate NoScope's Generation 1 Life cycle to last five years. Using the Stages in the Product Life Cycle (Figure 2.4), this would account for our introduction and growth period. While firmware updates will still be pushed through the end of the product's lifecycle, during the last two years, all hardware development will be shifted towards creating a second generation of NoScope.

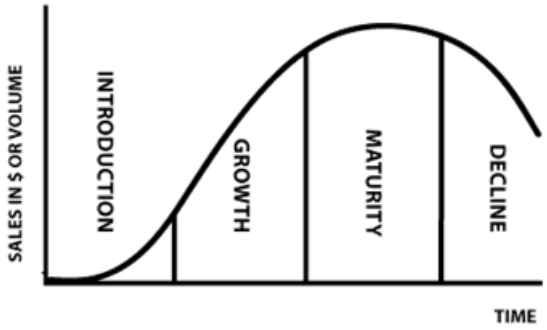

Figure 2.8: Product Life Cycle illustration Source: `https://serrvartisans.files.wordpress.com/2012/03/productlifecycle.gif`

The second generation will be slightly more economical, yet offer more features, such as automatic disease diagnosis and cloud storage services. At this point we will heavily push marketing and brand recognition, having built a stable user base with the first generation model. When NoScope extends from Growth to Maturity, our team will branch off into two distinct consumer products: a medical grade microscope for doctors and other professionals, and a consumer model suitable for schools and

affordable enough to be bought in bulk.

Further on, our company will form an R&D team to research future expansions and applications for our technology. When NoScope enters into the Decline portion of the life cycle, all efforts will be put towards commercializing R&D's prototypes. This may involve changing markets entirely (targeting maker/hobbyist fields instead of medical professionals) and will depend entirely on current market trends. We estimate the total time period from Introduction to Decline to be 10 years, following current market trends as well as the computational "Moore's Law" stating how computing power doubles approximately every 18 months, causing our product to become obsolete if we do not modify it.

4 References

Anderson A.,

Pelican Product, Inc. Hoovers.

http://subscriber.hoovers.com/H/company360/overview.html?companyId=138680000000000, Accessed March 1, 2015.

CellScope

2015. Oto Home. https://www.cellscope.com/household/buy_oto_home,

Accessed March 1, 2015.

Christensen, Clay. "Disruptive Innovation." Clay Christensen. http://www.claytonchristensen.com/key-concepts/

Accessed February 16, 2015.

Fleischer B,

2004. Editorial: 100 years ago: Giemsas solution for staining of plasmodia.

Tropical Medicine International Health 9: 755756. http://onlinelibrary.wiley.com/doi/10.1111/j.1365-3156.2004.01278.x/pdf

Accessed 15 February, 2015.

Griffith KS, Lewis LS, Mali S, Parise ME.

2007, Treatment of Malaria in the United States: A Systematic Review. Journal of American Medical Association.;297(20):2264-2277. doi:10.1001/jama.297.20.2264

http://jama.jamanetwork.com/data/Journals/JAMA/5164/jcr70004_2264_2277.pdf Accessed 15 February, 2015.

IndustryARC

2013. Global Microscopy Devices Market (2013 2018) By Types (Electron, Optical & Scanning Probe); By Components (Camera, CMOS Sensors, Display Screen, Lenses, Probe, Scanner, Staining Elements); By Applications (Physics, Chemistry, Forensic Science, Life Sciences, Material Sciences, Semiconductors) http://industryarc.com/Report/116/microscope-microscopy-devices-market.html

Isikman, S. O., Bishara, W., Sikora, U., Yaglidere, O., Yeah, J., & Ozcan, A.

2011. Field-portable lensfree tomographic microscope. Lab on a Chip, 11(13), 2222-2230.

http://pubs.rsc.org/en/content/articlepdf/2011/lc/c1lc20127a

Kak, A. C., & Slaney, M.

1988. Principles of computerized tomographic imaging (Vol. 33). Siam.

Lytro, Inc

2015. The First Generation Lytro Camera.

https://store.lytro.com/collections/the-first-generation-lytro-camera Accessed March 1, 2015.

Levoy, M., & Hanrahan, P.

1996, August. Light field rendering. In Proceedings of the 23rd annual conference on Computer graphics and interactive techniques (pp. 31-42). ACM.

http://doi.acm.org/10.1145/237170.237199

McWilliams, Andrew

2013. IAS017E - Microscopy: The Global Market. BCC Research. Accessed on 28 February, 2015.

http://www.bccresearch.com/market-research/instrumentation-and-sensors/microscopes-market-ias017e

html

Nikon Corporation.

2013. Nikon 2013 Annual Report.

http://www.nikon.com/about/ir/ir_library/ar/pdf/ar2013/13annual_e.pdf

Oliver, Lynett.

"NIKON CORPORATION." Hoover Company Profile

http://subscriber.hoovers.com/H/company360/overview.html?companyId=51742000000000.AccessedFebruar

2015.

Rosen, Shara, Steven Heffner, and LLC Information.

Cell-based Diagnostics: Technologies, Applications, and Markets. New York, N.Y.: Kalorama Information, 2005.

Sean C. Murphy, Joseph P. Shott, Sunil Parikh, Paige Etter, William R. Prescott, and V. Ann Stewart

The Gold Standard:Microscopy, in Malaria Diagnostics in Clinical Trials, American Journal of Tropical Medicine and Hygiene, 2013 89:824-839; Published online September 23, 2013, doi:10.4269/ajtmh.12-0675

http://www.ajtmh.org/content/89/5/824.full.pdf+html Accessed 15 February, 2015.

Singh, P., Sachs, J.D.

2013. 1 million community health workers in sub-Saharan Africa by 2015.

http://1millionhealthworkers.org/files/2013/01/1mCHW_article_Lancet_2013-03-29.pdf

Tadrous, P.J.

2011. Subcellular Microanatomy by 3D Deconvolution Brightfield Microscopy: Method and Analysis Using Human Chromatin in the Interphase Nucleus. Anatomy Research International, 28(7), 501503.

http://www.hindawi.com/journals/ari/2012/848707/

Tian, L., Wang, J., & Waller, L.

2014 .3D differential phase-contrast microscopy with computational illumination using an LED array. Optics Letters, 39(5), 13261329. 2014 March

http://ol.osa.org/abstract.cfm?URI=ol-39-5-1326

Uba, Tracy.

2015. "Carl Zeiss AG." Hoover Company Profile

http://subscriber.hoovers.com/H/company360/overview.html?companyId=59002000000000. Accessed February 10, 2015.

Ulama, Darryle

2014. IBISWorld Industry Report 33441a: Semiconductor & Circuit Manufacturing in the US. http://www.ibis.com, Accessed February 16, 2015.

Wongsrichanalai, Chansuda, Mazie J. Barcus, Sinuon Muth, Awalludin Sutamihardja, and Walther H. Wernsdorfer.

2007. "A review of malaria diagnostic tools: microscopy and rapid diagnostic test (RDT)." The American journal of tropical medicine and hygiene 77, no. 6 Suppl : 119-127.

http://www.ajtmh.org/content/77/6_Suppl/119.full.pdf+html Accessed 15 February, 2015.

World Health Organization (WHO)

2010: Clinical Disease and Epidemiology: Guidelines for the Treatment of Malaria, Second Edition http://whqlibdoc.who.int/publications/2010/9789241547925_eng.pdf Accessed 15 February, 2015

World Health Organization

2014. World Malaria Report 2014.

http://www.who.int/malaria/publications/world_malaria_report_2014/en/ Accessed February 16, 2015.

World Health Organization

2014b. Malaria Fact Sheet in WHO Media Centre

http://www.who.int/mediacentre/factsheets/fs094/en/ Accessed February 16, 2015.

A Return of Investment Calculations

Costs Calculation

	Year 1	Year 2	Year 3	Year 4	Year 5	Year 6
41900000	0	0	7876	23628	55132	118139	236278
Annual Sales:	0	0	0.1	0.3	0.7	1.5	3

Part #	Units per Part	Cost Per Part	Annual Cost	
ATtiny2313	1	0.745	$5,867.58	
HC595 Shift Reg	1	0.1108	$872.65	
LED Matrix	1	50	$393,796.99	
CMOS Camera	1	2.02	$15,909.40	
Camera Module	1	20	$157,518.80	
Housing	1	10	$78,759.40	**$652,724.82**

Part #	Units per Part	Cost Per Part	Annual Cost	
ATtiny2313	1	0.745	$17,602.73	
HC595 Shift Reg	1		$0.00	
LED Matrix	1	50	$1,181,390.98	
CMOS Camera	1	2.02	$47,728.20	
Camera Module	1	20	$472,556.39	
Housing	1	10	$236,278.20	**$1,955,556.48**

Part #	Units per Part	Cost Per Part	Annual Cost	
ATtiny2313	1	0.745	$41,073.03	
HC595 Shift Reg	1		$0.00	
LED Matrix	1	50	$2,756,578.95	
CMOS Camera	1	2.02	$111,365.79	
Camera Module	1	20	$1,102,631.58	
Housing	1	8	$441,052.63	**$4,452,701.97**

Part #	Units per Part	Cost Per Part	Annual Cost	
ATtiny2313	1	0.745	$88,013.63	
HC595 Shift Reg	1		$0.00	
LED Matrix	1	20	$2,362,781.95	
CMOS Camera	1	2.02	$238,640.98	
Camera Module	1	15	$1,772,086.47	
Housing	1	8	$945,112.78	**$5,406,635.81**

Page 1

Costs Calculation

Part #	Units per Part	Cost Per Part	Annual Cost	
ATtiny2313	1	0.745	$176,027.26	
HC595 Shift Reg	1		$0.00	
LED Matrix	1	20	$4,725,563.91	
CMOS Camera	1	2.02	$477,281.95	
Camera Module	1	15	$3,544,172.93	
Housing	1	8	$1,890,225.56	**$10,813,271.62**

Employee Costs	Engineers	Executives	Support Staff	Support Payroll
Year 1	5	0	0	$500,000.00
Year 2	3	2	2	$700,000.00
Year 3	6	2	3	$1,050,000.00
Year 4	6	2	5	$1,150,000.00
Year 5	8	2	7	$1,450,000.00
Year 6	13	2	10	$2,100,000.00

Page 2

ROI

ROI Period (yrs)	3					
Year	1	2	3	4	5	6
Total Costs:	$500,000.00	$1,352,724.82	$3,005,556.48	$5,602,701.97	$6,856,635.81	$12,913,271.62
Product Cost:	**$120.75**					
Product Cost (x1.5)	**$181.12**					

Part III

IP Strategy

1 Introduction

This portion of the report is not meant to be an exhaustive analysis on all possible forms of intellectual property protections. Instead, this is meant to be an extension on our business strategy in the previous section, and a brief outlook on the most pressing IP concerns that may aid or hamper us in NoScope's competitiveness in the microscopy arena.

The most unique and potentially patentable portion of our project is the hardware. Four main pieces comprise our system: the LED array and its controlling system, a sample holder, a camera sensor, and a moving stage to mount the sensor. In particular, it is the specific combination of these components that succinctly captures the three critical value propositions of our project: 3D imaging, lack of lenses, and super-resolution. Light from different, single LEDs will cast shifted images of a specimen directly on our CCD camera sensor, giving us the angular information we need to perform 3D reconstruction of the specimen. In addition, the moving stage allows us to translate the camera sensor in microscopic scales - this creates multiple shifted versions of a single image, allowing us to combine these images using super-resolution techniques to a higher resolution than our physical pixel would allow.

The reasons to focus on hardware patenting over image processing algorithms stem from concerns of practicality. First, most of the algorithms we use are based on already published work, precluding any sort of claim on them. Second, many of our competitors have successfully patented their hardware, and this sets a strong precedence for us to consider following the same route. Moreover, one of our close academic competitors from UCLA, which we have analyzed in the business strategy paper, has successfully patented a utility patent with USTPO.

However, the fact that the UCLA Ozcan group has filed a patent using a technology very similar to ours is also a cause of concern. In the next section, we will examine in detail, their group's patent, and demonstrate that our hardware does not infringe their claim. Finally, after establishing the viability of obtaining a patent, we will explain why team NoScope believes that, although obtaining a patent is crucial for getting the product to market, it will do little to maintain our competitive edge in the long-term.

2 Examining our Competitor's Patent

The name of the patent is "Lens-free wide-field super-resolution imaging device". Its schematic representation of the invention is shown in figure 1 below. In the abstract of the patent, the group describes their design as an imaging system with "an image sensor and a sample holder disposed adjacent to the image sensor" (Ozcan et al, 2014), which bears similarity to our design. Their design also includes "an illumination source configured to scan in two or three dimensions relative to sensor array" (Ozcan et al, 2014), which is also similar to our system. They included LEDs as one type of their illumination sources. In addition, they mentioned in the patent "the system includes least one processor configured to reconstruct an image of sample", similar to NoScope.

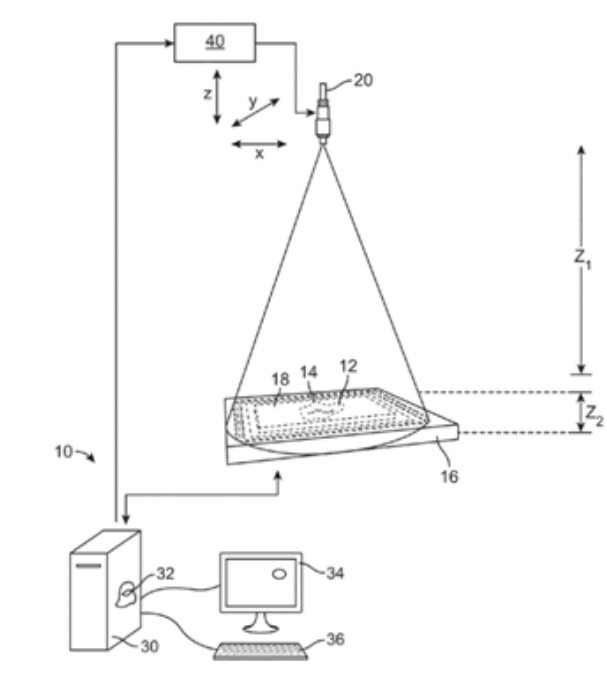

Figure 3.1: Schematic representation of invention of patent filed by Ozcan Research Group (Ozcan 2014, p3)

2.1 Their Five Claims

Although Ozcan's patent has many similarities to our own, there is no possibility of a successful lawsuit on their part due to key distinctions between their patent's claims and our product. Ozcan's patent has 29 claims (Ozcan et al, 2014), which serve to distinguish whether infringement has occurred. Of these 29 claims, there are five main ones with the rest being smaller elaborations to the "big five"

claims, e.g., different light sources or minor changes to the setup. The major claims are diagrammed below.

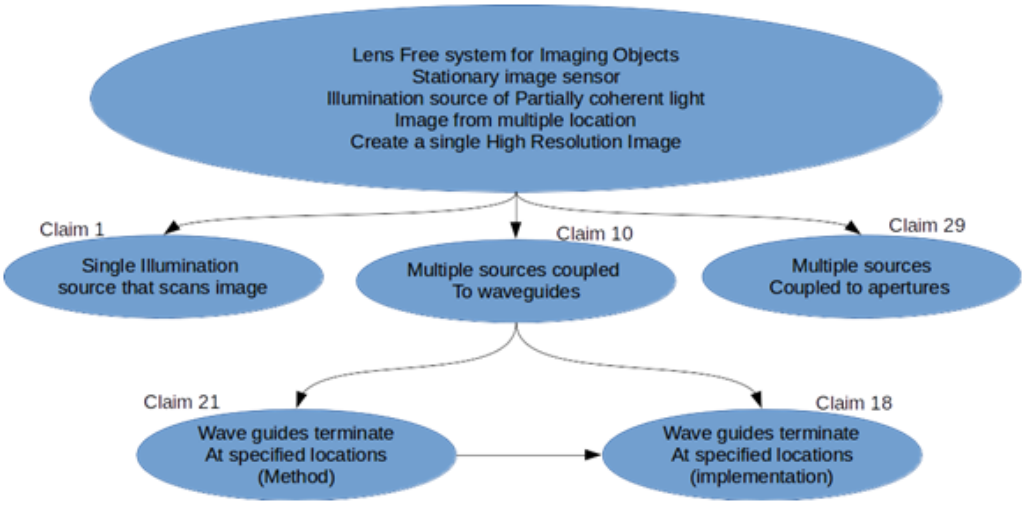

Figure 3.2: Summary of 5 major claims of Ozcan's lens-free microscope.(Ozcan 2014). Arrows connecting claims imply that the claim has all the features of it's parent claim, and additionally it's own sub-features.

To analyze whether our group would be in violation of these claims, each major claim was analyzed using the concept of "Doctrine of Equivalents", articulated in a classic Warner vs. Hilton law case as a test for whether a product violated the claims of a patent (Warner/Hilton, 1997). The Doctrine acts as a three point test. If a product "performs substantially the same function in substantially the same way to obtain the same result," (Warner/Hilton, 1997) it is in violation of the patent's claim. Fortunately for our group, while parts of Ozcan's claims perform substantially the same function in substantially the same way, none of them obtain the same result. Ozcan's patent exclusively covers the creation of a single high-resolution, or "super-resolution" image from a series of lower resolution images. Our group creates a 3D image of the object being imaged, and does not currently make any claims for super-resolution imaging, as we are limited by the resolution of our imaging device. This notable difference would make us exempt from any infringement claims Ozcan's group could make regarding their patent.

3 Competitive Advantage of a Patent

In our previous section, we examined one of our closest academic competitors, Ozcan Group of UCLA, and determined that it is indeed possible for us to file a similar hardware patent that would not infringe on any of their claims. In this section, we will examine the competitive advantages a patent confers in getting our product to market, and finally, make an overall recommendation on devising our intellectual property strategy.

3.1 Differentiation - Hallmark of Innovation

A key advantage of filing for a patent is that it acts as a key differentiating point for our product, especially in a technologically driven industry like microscopy. According to BCC, which performed a filtered search for on USPTO, a large company such as Olympus holds approximately 58 utility patents on optical microscopy (McWilliams 2013: 38). In pitting against ourselves against these large rivals in microscopy, a patent is almost a necessity in signifying technological innovation in our product.

In addition, patents are also vital for the process of raising capital if we were to begin as a startup company. For a startup with focus on selling a hardware device, a patent is not only a direct indication of innovation, it is also the assurance that we hold the legal right to produce and manufacture the product. Conversely, a lack of patent raises doubts from potential angels or venture capitalists looking to invest into NoScope. Obtaining a patent would be an unavoidable requirement if we wish to start a company around our lensless microscope.

3.2 Looking beyond the patent

However, beyond the practical purpose of securing funding and differentiating ourselves from our competitors, a patent will provide negligible long-term competitive advantage in the microscopy market. The first reason is that microscopy is by nature an international market. Filing for patent protection in multiple countries is both time-consuming and expensive. In traditional optical microscopes, the U.S. only accounts for 34% of the overall market (McWilliams 2013: 125). Moreover, as detailed in our strategy section, we are targeting malaria-endemic areas, which includes a considerable number of countries such as North India, and regions in Africa. Unfortunately, IP laws are only applicable in the country in which the patent is filed. Our lensless design will not be protected in our primary geographical market, and the financial resources required for multiple patent filings is prohibitive for

a new entrant like us.

Moreover, unlike what conventional wisdom would suggest, a patent in the microscopy market is unlikely to prevent competitors from producing similar, yet non-infringing designs. For imaging in microscopy, multiple ways of achieving the same function exist, many of which are based on well-established academic work, such as super-resolution. A clear example would be how we ourselves have circumvented UCLA's patent claims with a different illumination device, as well as using a moving sensor stage, in order to achieve similar functions of pixel super-resolution. Thus, it does seem reasonable to deduce that there will likely be potential competitors producing altered designs that can directly compete with NoScope.

Taking into consideration the above drawbacks, our group thus believes that obtaining a patent is a necessary step in order to bring the product to market. While it is necessary for raising capital in the early stages, a patent will not help us establish a monopoly in the malaria niche we segmented. This brings us back to our final point we made in our business strategy paper: a long term sustainable advantage in the microscopy market requires constant innovation, and a continually improving product.

References

McWilliams, Andrew

2013. IAS017E - Microscopy: The Global Market. BCC Research. Accessed on 28 February, 2015. http://www.bccresearch.com/market-research/instrumentation-and-sensors/microscopes-market-ias017e html

Ozcan Aydogan, Bishara Waheb

2014. Claims, in "Lens-free wide-field super-resolution imaging device" U.S. Patent 8,866,063, Oct 4, 2012. http://patft.uspto.gov/netacgi/nph-Parser?Sect1=PTO2&Sect2=HITOFF&p=1&u=%2Fnetahtml%2FPTO%2Fsearch-bool.html&r=2&f=G&l=50&co1=AND&d=PTXT&s1=lens-free&s2=ozcan&OS=lens-free+AND+ozcan&RS=lens-free+AND+ozcan

Tian, L., Wang, J., & Waller, L.

2014 .3D differential phase-contrast microscopy with computational illumination using an LED array. Optics Letters, 39(5), 13261329. 2014 March http://ol.osa.org/abstract.cfm?URI=ol-39-5-1326

Warner-Jenkinson Co. v. Hilton Davis Chemical Co

1997. US Supreme Court. Warner-Jenkinson Co. v. Hilton Davis Chemical Co., 520 U.S. 17, 117 S. Ct. 1040, 137 L. Ed. 2d 146 (1997). https://scholar.google.com/scholar_case?case=11676408400176174 84&hl=en&as_sdt=2006&scfhb=1

Part IV

Individual Technical Contribution

3D Tomographic Reconstruction: Modeling and Implementation

Contents

1 Introduction

NoScope is a computational imaging system; that is, it takes several images of a target object, and then recombines these images using various algorithms in order to form 2D and 3D images. My technical contributions center around one of these key algorithms for production of 3D images—tomography. Together with Longxiang Cui, our overall task is to formulate how the model of tomography fits with our unique system, and to implement this model in the form of a computer program written in MATLAB.

In order to enlighten readers unfamiliar with tomography, consider a common human experience—CT scans. CT (computed tomography) scanning refers to the process of using a medical scanning device to obtain 3D images of an object's interior, particularly for visualizing tissue and other structures inside a human being's body (Dugdale, 2015). Tomography is the physical and mathematical model that allows computers to take perhaps thousands of images of a single object from different angles, and then to estimate what the internal structure of the object truly looks like based on the synthesis of all these images (Kak and Slaney, 2001, pg. 1). CT scanners use X-ray radiation so that the light may pass through a human body in order to be captured by detectors on the opposite side of the person. Similarly, our system uses visible-spectrum light to illuminate a microscopic sample in order to capture images with our camera sensor. Since visible light tends to diffuse through the bodies of micro-scale objects and organisms, we may avoid using harmful wavelengths of light, such as X-rays, while retaining the properties necessary for tomography.

In particular, the contributions discussed in this section include i) formulation of the pixel transformation to relate real images to data useful to the tomography algorithm, and ii) implementation of the backprojection process necessary for object reconstruction. Each of these points will be further detailed later in the section. These contributions combined with the forward projection and detector transformation discussed by Longxiang Cui form the total model of tomography used in our system in order to produce 3D images. The other image

algorithm used in our system based on lightfields in handled by Zeyi Lee, while Ying Ou is responsible for the prototype setup and housing, and Ryan Frazier implemented the hardware and control system for the prototype. Ou and Frazier's work together comprises the prototype on which the raw images are taken.

2 Tomographic Methods in Literature

2.1 Theory

A fundamental tomographic reconstruction algorithm is presented by Feldkamp et al. in the paper "Practical Cone-beam Algorithm". Now commonly referred to as the FDK algorithm, this tomographic method made huge advances in practicality and efficiency in three-dimensional tomographic reconstruction at its time of writing in 1984, and uses a 3D "backprojection" to form the imaged volume (Feldkamp et al., 1984, p. 612). The FDK algorithm influences the papers we discuss next, and thus has been quickly introduced first.

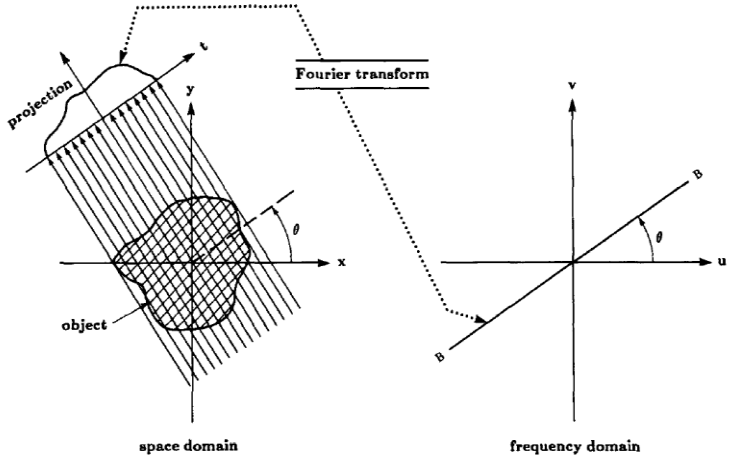

Figure 1: Parallel beam projection calculation (left) and the mapping of its transform to Fourier space (right) (Kak and Slaney, p. 57).

Kak and Slaney detail the various models of tomography that apply to different imaging systems in "Principles of Computerized Tomographic Imaging", and altogether give a strong overview of most of the relevant research in the field. This book provides a thorough analysis of these models from a theoretical as well as practical standpoint, giving significant insight regarding implementation of the core algorithms. Furthermore, Kak and Slaney tie these algorithmic details back to the underlying theory of the Fourier Slice Theorem nicely.

All models of tomography draw on a central signal processing result known as the Fourier Slice Theorem, which states that the Fourier transforms of all line integral projections through an object may be re-arranged in 2D such that the inverse Fourier transform of the 2D image is exactly the original, spatial-domain image of the object (Kak and Slaney, 2001, p. 56). In other words, one may take images using penetrative light sources in order to approximate the density

of the object along given lines (i.e., the projections), and subsequently reconstruct an image of the object—including its internal structure—by using Fourier methods (Kak and Slaney, 2001, p. 49). Figure 1 shows an example of the Fourier Slice Theorem being applied to an object. The projection calculation is carried out with parallel beams across the object, and this projection data is then transformed and mapped to the Fourier domain at the same angle at which the projection was taken in spatial domain (Kak and Slaney, 2001, p. 57).

The precise details of implementing tomography for a given imaging system depend on the formation of its projection data, which arises from the system's geometric characteristics (Kak and Slaney, 2001, p. 49). The categories of models are parallel beam, fan beam (equiangular or equally-spaced collinear), and cone beam (Kak and Slaney, 2001, p. 60, 77, 86, 99). Categories may differ based on the setup of the detector array as well as whether the source's rays are parallel or diverging. Figure 2 shows the setup of a cone-beam imaging system as well as the physical details of projection formation (Scherl et al., 2007, p. 3). The FDK algorithm applies to this type of setup.

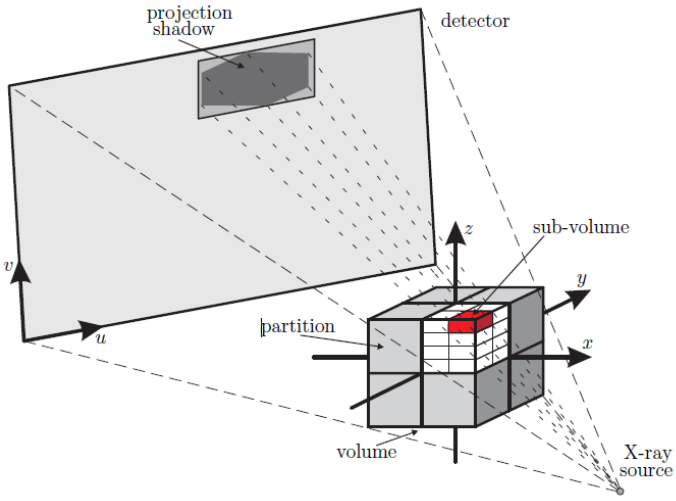

Figure 2: Cone-beam projection by an X-ray source. The object space is broken down into voxels to be assigned values during the reconstruction (Scherl et al., 2007, p. 3).

2.2 Types of Algorithms

Although "Principles of Computerized Tomographic Imaging" provides a rigorous mathematical and theoretical foundation for tomography, it fails to appeal much to intuition while also leaving out details regarding application to real images. Zhang et al. compare various advanced methods of improving tomographic image quality in "A Comparative Study of Limited-Angle Cone-beam

Reconstruction methods for breast Tomosynthesis", and also detail the relationship of the aforementioned line integrals/projections to the raw image data.

Zhang et al.'s paper compares four algorithms for cone-beam reconstruction with limited angles. These algorithms include "backprojection algorithms, transform algorithms, algebraic reconstruction techniques, and statistical reconstruction algorithms" (Zhang et al., 2006, p. 3). Backprojection—the method detailed in Kak and Slaney's paper—is shown more intuitively in Zhang et al.'s paper. 3D tomography involves an inverse problem whereby 2D images are formed from the 3D object by a known process, but recombination of the images into the 3D object is not exact due to the limited number of angles from which to acquire images. In Zhang et al., the space to be reconstructed is broken down into an arbitrary number of voxels. For each projection that passes through a voxel, the portion of that projected ray through the voxel is added to the voxel, and then voxels are normalized by the total path length of all rays passing through each one (Zhang et al., 2006, p. 4). Essentially, each projection value (derived from a pixel value of one image) is smeared evenly back across the line along which the projection's line integral was calculated (Zhang et al, 2006, p. 4).

The tomographic model requires one more detail: relating the pixel values of the raw images to the projection values used in the computation. Intuitively, a darker pixel value in a raw image implies that the light traveling to that pixel experienced more attenuation, and thus the path the light traveled from the source to the pixel must be either longer or made of denser material. With this understanding of the pixel values, the projection values (used for computation) may be derived from the pixel values through

$$y = k \ln\left(\frac{I_o}{I_i}\right) \qquad \text{Eq. 1}$$

where y is the projection value corresponding to a pixel receiving intensity I_o from a source ray with intensity I_i, and where k is a constant of proportionality (Zhang et al., 2006, p. 3).

2.3 Similar Systems

Next, a successful implementation of tomography in a microscopic system is considered in a paper presented by Isikman et al. titled "Lens-free Optical Tomographic Microscope with a Large Imaging Volume on a Chip". Isikman et al. have achieved a 3D-capable microscope by combining the results of pixel superresolution techniques with the reconstruction capability of tomography (Isikman, 2011, p. 1). An important development that this paper demonstrates is the use of tomography with multiple axes to cover a greater range of angles and thus to obtain a better reconstruction (Isikman, 2011, p. 2). Whereas more typical setups use a source rotating about an object along one axis (think of the axis through the tube of a CT scanner), tomographic reconstruction may be improved by rotating the light source along multiple axes, as seen in Figure 3. This added degree of freedom ameliorates the issues in reconstruction quality caused by the information loss of a limited range of angles due to the geometric setup of the system.

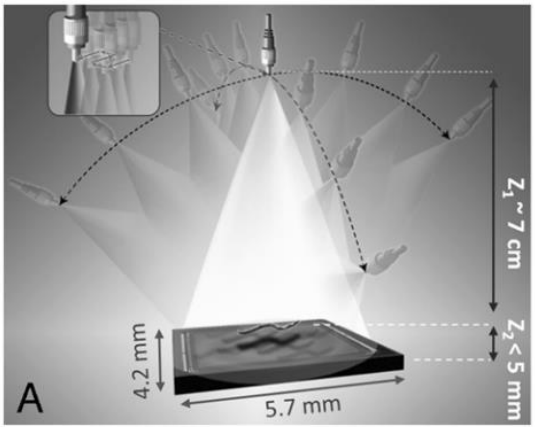

Figure 3: Multiple-axis tomography. The light source (top of image) rotates about the imaging plane in multiple directions for improved quality (Isikman, p. 2).

The information from the preceding papers lays the groundwork for developing a tomographic model for our system. By considering the geometry and end goals of our system, a projection model (parallel beam, fan beam, or cone beam) may be chosen, and the reconstruction may be achieved through an algorithm such as backprojection by converting raw pixel values into projection data. NoScope's requirements in particular require more than simple application of pre-existing models, however; our system's geometry necessitates dealing with sources of non-ideality not present in these discussed models in order to capture the value of tomographic imaging in an entirely new way.

3 Tomographic Model Formulation

3.1 Requirements

In order to achieve the desired 3D imaging capability, a tomographic model must be developed for our unique system. In the preceding section, several projection schemes and reconstruction models were covered. After considering our physical setup and end goals for the produced images, the most appealing model is a cone-beam projection scheme with two-dimensional scanning combined with a filtered backprojection reconstruction.

The choice of a cone-beam projection scheme stems from two factors: the use of a divergent light source, and the configuration of the detectors. A strong motivating force in NoScope is inexpensive parts, which fuels our decision to use of a simple LED array and a generic CCD camera sensor. The divergent nature of light from LEDs rules out the possibility of a parallel projection scheme. Furthermore, since NoScope uses a 2D detector, computational efficiency mandates the use of cone-beam projections, since one exposure makes use of all pixels in the sensor, whereas fanbeam geometries would only make use of one line of sensors. Simplicity and potential improvement constitute the main advantages of using a filtered backprojection for reconstruction. The algorithm is among the simplest reconstruction algorithms, and is often used as a baseline for more complicated reconstructions (Zhang et al., 2006, p. 1).

However, NoScope's configuration introduces some non-idealities that must be accounted for in the model. Perhaps the largest obstacle is the tilted detection plane. Tomography almost always relies on a sensor that moves with the source such that the relative positions of the sensor and the detector are constant. Our system, similar to that proposed by Isiman et al., lacks this perpendicular detection plane. This introduces two problems: light intensity drops off due to the angle of incidence on the CCDs, and all images become skewed as the projection is stretched across the imaging plane, causing the image to no longer reflect the actual structure of the object. Furthermore, the LEDs do not point directly at the center of the object, resulting in a

loss of intensity due to the LED characteristics that may be measured as a function of the offset angle (Ou, 2015, p. 8).

For the problem of skewed images, fellow NoScope team member Longxiang Cui proposes a transformation of the projection data based on the angle the light hits the detection plane, which is derived from the location of the illuminating LED (Cui, 2015, p. 7). This transformation re-adjusts the raw data as if it were originally imaged with a perpendicular detection plane.

3.2 Pixel Intensity Adjustment Model

The light drop-off occurs due to three sources: the LED characteristics, the angle of incidence on the sensor array, and intensity falloff with distance. The first factor has been quantified for our system and is given approximately by

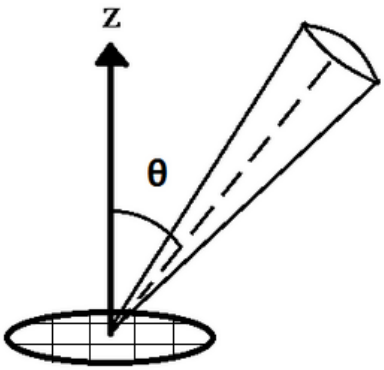

Figure 4: LED array (bottom plane) emitting light in a solid angle at angle θ from the perpendicular.

$$\alpha = \cos(1.2\theta) \qquad \text{Eq. 2}$$

where α is the fraction of light emitted and θ is the angle from the center line of the LED of the line from the LED to the object's center, as shown in Figure 4 (Ou, 2015, p. 8).

The second factor occurs when the incident light on a CCD falls off due to the effective surface area of the CCD when tilted, as shown in Figure 5 in 2D. By simple geometry, the effective area A_{eff} is given by

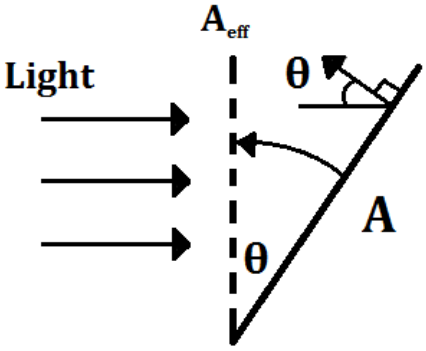

Figure 5: Effective surface area of a CCD with incident light at an angle of θ.

$$A_{eff} = \mathrm{A}\cos(\theta) \qquad \text{Eq. 3}$$

Since a CCD outputs a value proportional to the incident intensity, the pixel values in the projected images fall off by the ratio of A_{eff} to A, i.e., cos θ.

The last factor in the adjustment model accounts for the drop in field density as the distance from a source increases. This is a result of conserving the total energy of a field across a surface equidistant to an emitter, and is an instance of the commonly known inverse square law whereby

$$I \propto \frac{1}{r^2} \qquad \text{Eq. 4}$$

where I is the field strength (in this case intensity) and r is the distance from the source. Thus, given an intensity I_o at some distance d, a second intensity I at a distance x is given by

$$I = I_o \left(\frac{d}{x}\right)^2 \qquad \text{Eq. 5}$$

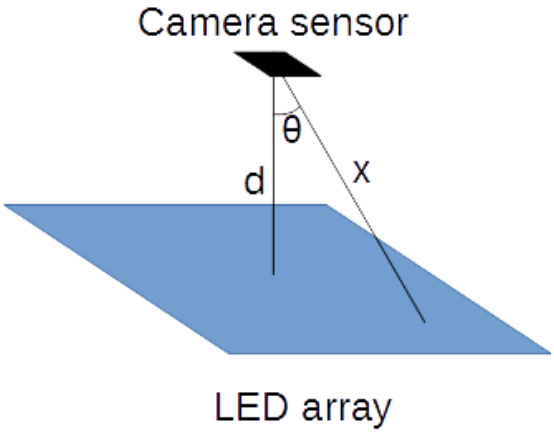

Figure 6: Geometric setup showing path length differences between the camera sensor and different LEDs as related by the central angle θ.

Applying Eq. 5 to our setup as shown in Figure 6, and noting that cos θ = d/x, we see that the adjustment factor is given by $\cos^2 \theta$.

Combining these results in Eq. 2 through Eq. 5 with Eq. 1, every pixel value i in an image taken at angle θ from the central line of the system (middle LED to object) must be adjusted to a projection value p through the formula

$$p = -\ln\left(\frac{i}{k\,cos^3(\theta)\,cos(1.2\theta)}\right) \qquad \text{Eq. 4}$$

Note that this formula is applied to every pixel of the image, which makes the approximation that the angle from the current LED to the middle sensor pixel is the same as the angle from the current LED to any other sensor pixel. This is possible due to the camera sensor's small size. Lastly, the parameter k may be set equal to 1, as it simply represents a linear scaling of the resulting voxel values in the reconstruction, i.e., brightening or dimming the 3D image.

3.3 Implementation of the Filtered Backprojection

Having formulated the tomographic model, the computer implementation may be coded. The implementation was aided by a pre-existing implementation of the filtered backprojection with a standard geometry by Kyung Sang Kim available for free use under a BSD license (Kim, 2015). The advantages conferred by reuse of fractions of this program include helping set up the geometric parameters necessary to define our setup, the implementation of the projection filtering, and the implementation of the backprojection, but with only one axis of rotation.

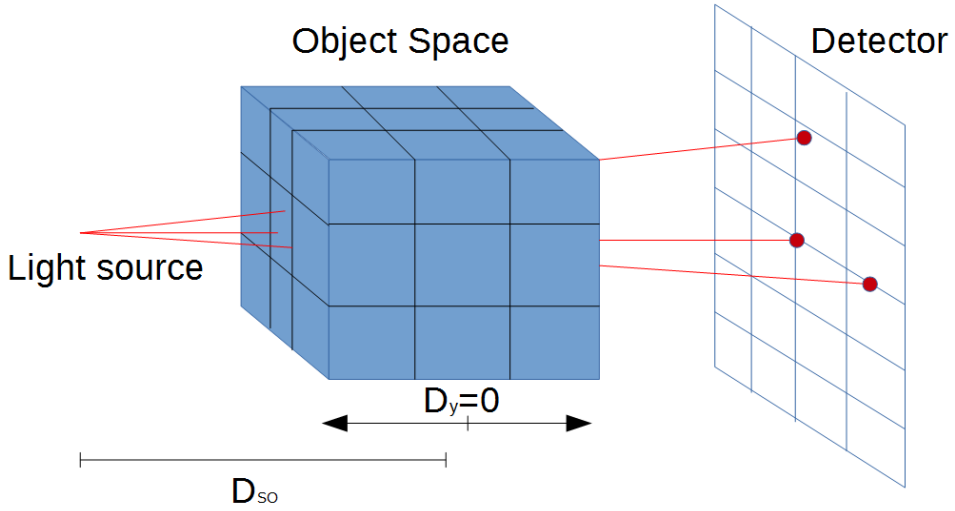

Figure 7: Ray tracing through three example voxels (blue) to find the corresponding points on the detection plane (red dots). The detection plane has a grid of values supplied by the projection data. These values are linearly interpolated in 2D to find the values at the red dots. D_{SO} is the distance between the source and object center, and D_y is the distance from the center of the object to a given voxel, which is used in the tracing process.

In order to implement the backprojection for our system, a 3D parametrized algorithm must be developed, whereas the starting point provided by Kim is 2D (Kim, 2015). We first perform a 3D rotation of the object's coordinate system to align its voxels with the center projection line of the system. Next, for each projection image, we map each voxel to its corresponding position on the projection image by tracing a ray through the voxel to the detection plane. An interpolation on the detection plane maps the existing projection values to the points indicated by the voxels, and these interpolated values are smeared back across the object, as shown in Figure 7. This process is repeated for every projection image, and the reconstruction is finished once all the smeared values are summed for every voxel.

4 Results and Discussion

4.1 Pixel Intensity Adjustment Results

Plotting the proposed model of light falloff against the attenuation calculated from blank images without a sample reveals a discrepancy not accounted for in the model. Although the proposed model follows the data for small angles, Figure 8 shows a more drastic falloff with greater angles. This may be due to the structure of the CCD array itself; as the angle of incident light becomes more extreme, some light is blocked from reaching each CCD by the physical edges surrounding each cell, resulting in a sharp falloff that is difficult to predict. Furthermore, the model did not take into account reflectance of the CCDs.

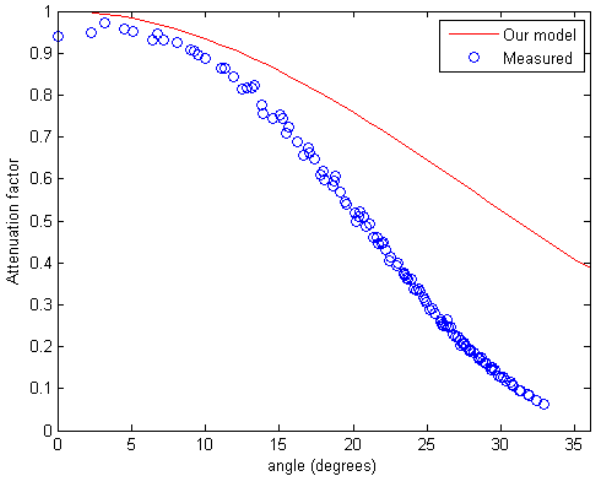

Figure 8: Light falloff vs. angle from center. The measured falloff was calculated by taking the averages of blank images at various illumination angles.

To account for this imparity between the model and the data, the light falloff may be calculated more directly from the prototype's images. For each LED, a map of its lighting pattern may be obtained from an image with no sample. In order to derive the pattern from the raw image, some processing is needed to remove the extraneous features caused by dirt on the equipment and sample. The algorithm used for this task breaks the image into 25 sub-images, applies a local thresholding based on the local average pixel value, and then re-combines the sub-images and applies a large average filter. With this lighting pattern, the raw images may be adjusted on a pixel-by-pixel basis to negate the effects of both the light falloff with angle from the center as well as the uneven lighting in a single image. To accomplish this, each pixel value in a given sample image is divided by the ratio of its corresponding pixel value in the lighting pattern to

255, which we use as the ideal pixel value in a full, even illumination. An example of the results obtained from this algorithm is shown in Figure 9.

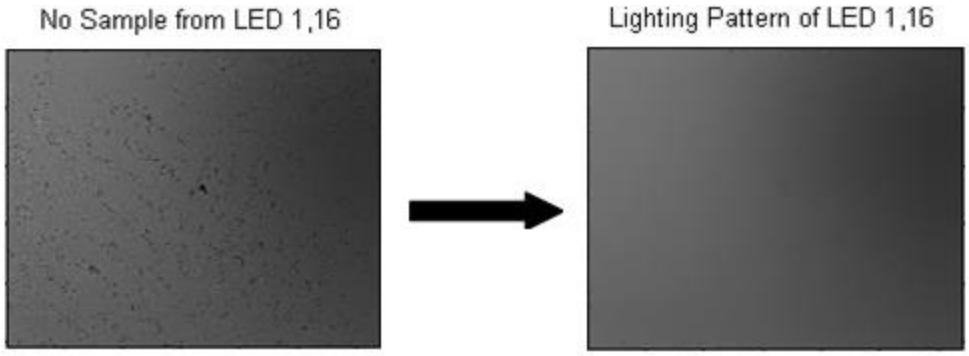

Figure 9: A blank image taken from LED with coordinates (1,16) on the LED grid, and its corresponding illumination pattern obtained after processing with the local thresholding algorithm.

Figure 10 shows an example of the pixel adjustment performed on a sample image of *ctenocephalides*. The raw image is essentially a shadow cast by the object, which explains the dark center and light background. This is transformed to the second image, where the pixel values now represent density, or line integrals, through the object along the light's path, hence the denser regions being represented by higher intensities. Note that the uneven background illumination has been eliminated.

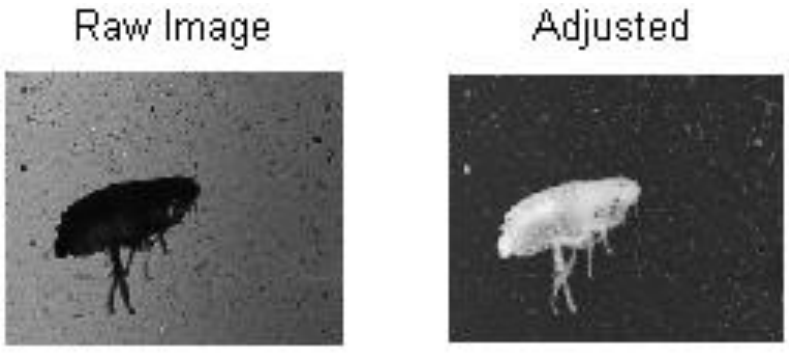

Figure 10: Pixel adjustment example run on an image of *ctenocephalides*.

4.2 3D Reconstruction Results

To determine reconstruction results, we simulated reconstruction of various spheres using a geometric setup identical to the real prototype. Longxiang Cui has developed a forward projection algorithm to simulate capturing the raw images, which is used for all simulations (Cui, 2015, p. 8). The forward projection is also useful for future improvements to the reconstruction, such as with an iterative reconstruction approach (Mishra et al., 2004, p. 1524).

Simulated reconstruction results for the central slices of various spheres are shown in Figure 11. Images (a) and (b) are the central slices of the reconstructed volume of a single sphere taken at 90 degrees to one another. In (b), the horizontal axis corresponds to the axis between the source and detector, which we expect the smearing to occur across due to the missing angles. Intuitively, this smearing arises due to the lack of definitive edges available on the borders of the circle in the projection images.

Images (c) and (d) of Figure 11 both depict results of reconstructing two adjacent spheres. In (c), the source-detector axis is directed out of the plane, which gives definition to the gap between the spheres. However, (d) shows the reconstruction result if the entire sample is rotated 90 degrees such that the source-detector axis passes through both spheres. In this case, the algorithm fails to make a strong distinction between the two spheres due to the overlap of the smeared regions.

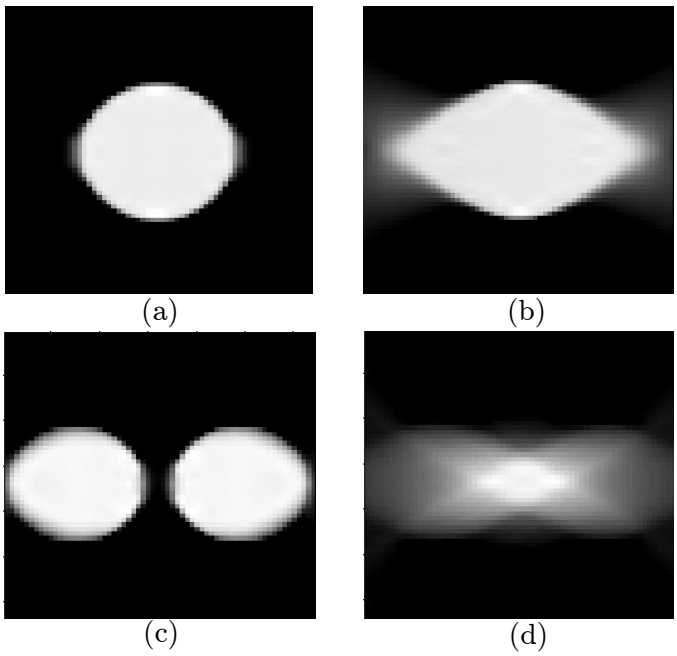

Figure 11: Simulated reconstruction results for central slices of spheres. (a) Forward-facing central slice of single sphere. (b) 90° rotation of image (a). (c) Two spheres with source-detector axis out of the page. (d) Two spheres with horizontal source-detector axis.

Reconstruction results run on the *ctenocephalides* sample are displayed in Figures 12 and 13. The central slice in Figure 12 provides decent detail, including features such as the cavities in the body and structure of the legs. However, as the focus moves from the center of the object, the

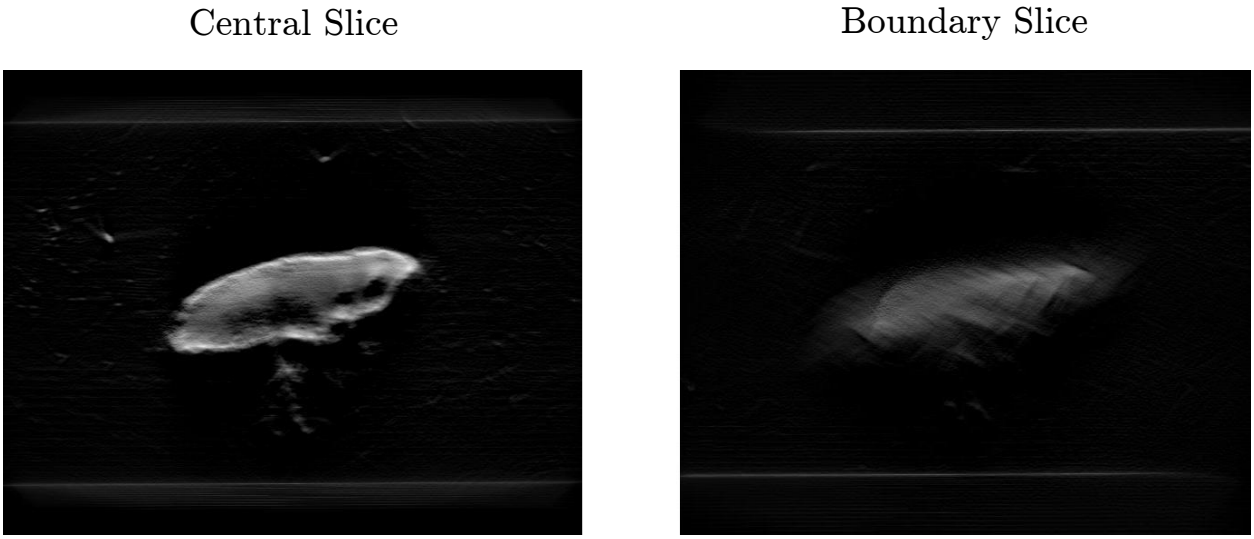

Figure 12: Reconstructed slices of a flea through the central slice (left) and a slice on the edge of the object (right).

reconstruction quality declines to that shown in the boundary slice in Figure 12. This is due to the same missing angles phenomenon that caused the smearing in Figure 11, but is more pronounced due to the difficulty in adjusting the raw images to a parallel, centered imaging plane as well as the decrease in signal-to-noise ratio for images taken by LEDs toward the outside edges of the array, which effectively further reduces the available range of angles. The 3D reconstruction's surface is shown in Figure 13.

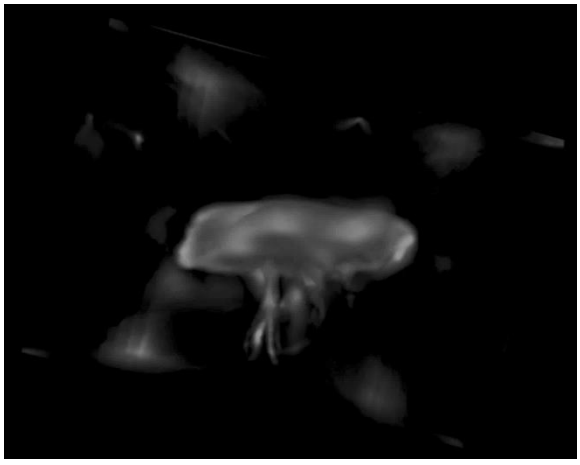

Figure 13: Surface of reconstructed volume.

References

Cui, Longxiang. 2015. Technical Contributions.

Dugdale, David C. "CT Scan." US National Library of Medicine. http://www.nlm.nih.gov/medlineplus/ency/article/003330.htm. Accessed March 16, 2015.

Feldkamp, L. A., L. C. Davis, and J. W. Kress. "Practical Cone-beam Algorithm." 1984. Journal of the Optical Society of America A, 1(6), 612. http://dx.doi.org/10.1364/JOSAA.1.000612. Accessed April 14, 2015.

Isikman, S. O., Bishara, W., Sikora, U., Yaglidere, O., Yeah, J., & Ozcan, A. 2011. Field-portable Lens-free Tomographic Microscope. Lab on a Chip, 11(13), 2222-2230. http://pubs.rsc.org/en/content/articlepdf/2011/lc/c1lc20127a. Accessed March 16, 2015.

Kak, A. C., and Malcolm Slaney. *Principle of Computerized Tomographic Imaging*. Society of Industrial and Applied Mathematics, 2001.

Kim, Kyung Sang. "3D Cone Beam CT (CBCT) Projection Backprojection FDK, Iterative Reconstruction Matlab Example." Mathworks. March 10, 2012. Accessed March 16, 2015. http://www.mathworks.com/matlabcentral/fileexchange/35548-3d-cone-beam-ct--cbct--projection-backprojection-fdk--iterative-reconstruction-matlab-examples.

Mishra, Debasish, Jon P. Longtin, Raman P. Singh, and Vishwanath Prasad. 2004. "Performance Evaluation of Iterative Tomography Algorithms for Incomplete Projection Data." Applied Optics, 43(7) , 1522-532. http://dx.doi.org/10.1364/AO.43.001522. Accessed April 13, 2015.

Ou, Ying. 2015. Technical Contributions.

Scherl, H., Koerner, M., Hofmann, H., Eckert, W., Kowarschik, M., Hornegger, J. "Implementation of the FDK Algorithm for Cone-Beam CT on the Cell Broadband Engine Architecture." Proceedings of SPIE Medical Imaging 2007: Physics of Medical Imaging, 651058. Accessed March 16, 2015.

Zhang, Y., Chan, H.-P., Sahiner, B., Wei, J., Goodsitt, M. M., Hadjiiski, L. M., … Zhou, C. 2006. A comparative study of limited-angle cone-beam reconstruction methods for breast tomosynthesis. Medical Physics, 33(10), 3781–3795. doi:10.1118/1.223754. Accessed March 16, 2015.

Part V

Concluding Reflections

Concluding Reflections

NoScope as is still constitutes a novel and productive venture into a commercial, microscopic computational imaging system. However, upon conclusion of the project, the 3D tomographic reconstruction remains working only as a simulation. Development of the theoretical model was successful, but application to real data—the original goal of this task—still proves troublesome. Since tomography constitutes one of many of NoScope's computational methods, we are still able to produce 3D images in accordance with our original goal. In broader project context, conversion to a standalone product still requires significant work to reduce cost of key components, to increase portability of the software by means of alternate language implementations, and to create a more robust and portable housing structure. This gap between prototype and product is natural and was expected by the team.

Throughout this project, I gleaned several strategies and insights regarding project management in terms of coordinating with others, communicating information and ideas, and tracking project progress. The team felt highly disjointed and individual the first semester, and our communication suffered. We met only once a week as a group with our adviser, which largely served as a venue to communicate results. In response to this disjointed feeling, we scheduled a second weekly team meeting with a less stringent agenda that allowed us to speak more openly and facilitated more frequent communication of needs and obstacles that we experienced during our tasks. Furthermore, I learned to manage sharing a task with a team member. Both working on tomography, Longxiang Cui and I began meeting on a weekly basis to plan out our task, to work on development, and to combine results of individual sub-tasks. Altogether, more frequent meetings gave more opportunities to communicate, which allowed the team to function more effectively. Lastly, I learned the value of intermittently evaluating project progress and forming status updates. This provided a clear perspective to the team of the tasks that were lagging as well as the severity of the progress deficit, and spurred further work on those tasks and in some cases a re-structuring of the task in order to bump it forward on the timeline, e.g., cutting features to reduce development time.

NoScope currently provides an ingenious and simple method of imaging, but much more improvement may be made both in the signal processing as well as the physical prototype. The tomographic imaging results currently suffer from the well-known limited-angle problem. In order to improve the quality of the images, two different but not exclusive options may be pursued: physically restructuring the system, and applying more sophisticated limited-angle reconstruction algorithms. If a cost-effective method of developing a dome-shaped LED array were produced, a much larger range of angles would be made available for the digital reconstruction while preserving our price point. Additionally, many options exist in literature for improving reconstruction with a limited angular range with tomography, as mentioned in the literature review. Numerous algorithmic options have yet to be explored for this system (SART, ML-convex, etc.). Altogether, NoScope provides a promising platform for future development.